Implementation and Evaluation of the Dynamic Smagorinsky Model and an Eddy Dissipation Model with Multiple Reaction Time Scales in FireFOAM

G. Maragkos, T. Beji, and B. Merci
Georgios.Maragkos@UGent.be
Department of Flow, Heat and Combustion Mechanics, Ghent University
Sint-Pietersnieuwstraat 41, B-9000, Ghent, Belgium

Abstract
The implementation of the dynamic Smagorinsky model and an Eddy Dissipation Model (EDM) with multiple reaction time scales in the CFD code FireFOAM is presented and the newly implemented models are evaluated against two well-characterized experimental test cases: Shabbir's (1994) experiments on a turbulent buoyant plume and McCaffrey's (1979) experiments on small-scale fire plumes (14.4-57.5 kW). Overall, the numerical results show very good qualitative and quantitative agreement when compared to some of the standard models available in the code, for both the experimental test cases considered. These developments aim to supplement the available models of FireFOAM and to enhance the code's predictive capabilities of simulating fire-related scenarios.

Introduction
Detailed knowledge of the behavior and the dynamics of fires is essential for fire safety engineers working on everyday life applications, involving fire detection, fire suppression and venting, design of smoke control systems, fire heating of structural elements of buildings or thermal radiation hazards. CFD models can be used not only to evaluate the effectiveness of current or future fire protection systems, but also to answer `what if' questions and be used towards a cost-effective design without compromising fire safety in buildings [1]. A deeper understanding of the capabilities and limitations of the available CFD codes used for performing numerical simulations of fire-related problems will provide the fire safety engineers with the appropriate guidelines to carefully design and perform their CFD analysis when evaluating fire safety systems in buildings and industrial facilities. Within this framework, accurate modeling of the physics in the gas, liquid and solid phases is essential and a prerequisite for performing reliable simulations of fire scenarios involving complex physical processes such as pyrolysis, flame spread and interaction of fire with sprinklers. A key aspect towards performing reliable numerical simulations of fire applications is to accurately model turbulence, combustion and their interaction. If `static' models are applied in numerical simulations, calibration of model constants is often necessary, particularly if coarse meshes are used. Therefore, the use of dynamic models is preferable, because then no calibration process is needed before simulating new fire scenarios.

The main objective of the current study is to report on the implementation of new gas phase models (turbulence and turbulence-chemistry interaction) in the CFD code FireFOAM and to evaluate these newly implemented models against well-characterized experiments in literature. More specifically, the dynamic Smagorinsky model as proposed by Moin et al. [2] is applied to model turbulence, in which the model constant varies in both time and space. The implementation of a truly dynamic model is a significant improvement compared to the static models (e.g., one-equation, constant Smagorinsky, WALE) that are currently available in FireFOAM. In addition, the Eddy Dissipation Model (EDM) [3], used to model the turbulence-chemistry interactions, is extended by considering a simple reaction time scale

model for under-resolved fire dynamics [4]. This work aims at expanding the number of gas phase models available in FireFOAM and potentially enhance its predictive capabilities by evaluating the newly implemented models against well-known test cases. As such, Large Eddy Simulations (LES) are conducted with FireFOAM (version 2.4.x) and the newly implemented models are evaluated against the experiments by Shabbir et al. [5] (Case 1), involving a turbulent buoyant plume, and the experiments by McCaffrey et al. [6] (Case 2), involving small-scale CH_4 fire plumes with HRR varying between 14.4-57.5 kW. The present study is an extension of the previously conducted numerical work by Wang et al. [7] on McCaffrey's experiments.

Governing equations

FireFOAM, developed by FM Global, is an object oriented, C++-based, transient solver for fires and turbulent diffusion flames based on the OpenFOAM platform. FireFOAM version 2.4.x employed in the current study, uses a Favre-filtered fully compressible flow formulation and solves for the Navier-Stokes equations, along with transport equations for species mass fractions and sensible enthalpy [8]:

$$\frac{\partial \bar{\rho}}{\partial t} + \nabla \cdot \left(\bar{\rho} \tilde{u} \right) = 0 \tag{1}$$

$$\frac{\partial \left(\bar{\rho} \tilde{u} \right)}{\partial t} + \nabla \cdot \left(\bar{\rho} \tilde{u} \tilde{u} \right) = -\nabla \bar{p} + \nabla \cdot \left[\left(\mu + \mu_{sgs} \right) \left(\nabla \tilde{u} + \left(\nabla \tilde{u} \right)^T - \frac{2}{3} \left(\nabla \cdot \tilde{u} \right) I \right) \right] + \bar{\rho} g \tag{2}$$

$$\frac{\partial \left(\bar{\rho} \tilde{Y}_k \right)}{\partial t} + \nabla \cdot \left(\bar{\rho} \tilde{u} \tilde{Y}_k \right) = \nabla \cdot \left[\bar{\rho} \left(D_k + \frac{\nu_{sgs}}{Sc_t} \right) \nabla \tilde{Y}_k \right] + \overline{\dot{\omega}_k^{'''}}, \quad k = 1, ..., N_s - 1 \tag{3}$$

$$\frac{\partial \left(\bar{\rho} \tilde{h}_s \right)}{\partial t} + \nabla \cdot \left(\bar{\rho} \tilde{u} \tilde{h}_s \right) = \frac{D \bar{p}}{D t} + \nabla \cdot \left[\bar{\rho} \left(\alpha + \frac{\nu_{sgs}}{\mathrm{Pr}_t} \right) \nabla \tilde{h}_s \right] - \nabla \cdot \overline{\dot{q}_r^{''}} + \overline{\dot{q}_c^{'''}} \tag{4}$$

where $\overline{\dot{q}_c^{'''}} = \Delta H_c \cdot \overline{\dot{\omega}_F^{'''}}$, assuming complete combustion. The code assumes equal species diffusivities and unity Lewis number, hence, calculates only the thermal diffusivity which is expected to be more important than mass diffusivity in the case of fire applications. For all the cases in the paper, a value of $\mathrm{Pr}_t = 0.7$ has been used.

The dynamic viscosity is temperature-dependent and calculated by Sutherland's law [9]:

$$\mu = \frac{A_s \sqrt{T}}{1 + T_s / T} \tag{5}$$

where $A_s = 1.67212 \times 10^{-6}\ kg/(m.s.\sqrt{T})$ and $T_s = 170.672\ K$ are the two Sutherland coefficients.

The thermal diffusivity is expressed as:

$$\alpha = \frac{\lambda}{c_{pv}} \tag{6}$$

where c_{pv} is the heat capacity at constant pressure/volume and λ is the thermal conductivity calculated by the Eucken model [10]:

$$\lambda = \mu c_v \left[1.32 + \frac{1.77R}{c_v} \right] \tag{7}$$

where c_v is the heat capacity at constant volume and R is the gas constant. The heat capacities are temperature-dependent and are calculated based on the 7-coefficient NASA polynomials (Burcat Database) [11].

In the newly implemented dynamic Smagorinsky model [2], the sub-grid scale (sgs) viscosity is calculated as:

$$\mu_{sgs} = \bar{\rho} \left(c_s \Delta \right)^2 \left| \tilde{S} \right| \tag{8}$$

where $\left| \tilde{S} \right| = \left(2\tilde{S}_{ij}\tilde{S}_{ij} \right)^{1/2}$, $\tilde{S}_{ij} = 0.5\left(\nabla\tilde{u} + \nabla\tilde{u}^T \right)$ and $\Delta = (\Delta x \Delta y \Delta z)^{1/3}$ is the filter size with Δx, Δy and Δz the effective grid mesh spacings. The Smagorinsky constant is determined dynamically and varies locally in space and time as:

$$c_s^2 = \frac{\left\langle L_{ij} M_{ij} \right\rangle}{\left\langle M_{ij} M_{ij} \right\rangle} \tag{9}$$

where the brackets correspond to averages computed as local averages of their face values. The Leonard term is calculated as $L_{ij} = \bar{\rho}\tilde{u}_i\tilde{u}_j - \left(\overline{\rho u_i}\,\overline{\rho u_i} \right) / \bar{\rho}$, $M_{ij} = \beta_{ij} - a_{ij}$, $\beta_{ij} = -2\Delta^2 \bar{\rho} \left| \tilde{\tilde{S}} \right| \left(\tilde{\tilde{S}}_{ij} - \delta_{ij}\tilde{\tilde{S}}_{kk} / 3 \right)$ and $a_{ij} = -2\Delta^2 \bar{\rho} \left| \tilde{S} \right| \left(\tilde{S}_{ij} - \delta_{ij}\tilde{S}_{kk} / 3 \right)$. The hat denotes the use of a test filter of characteristic width $\Delta = 2\Delta$ while $\tilde{\tilde{f}} = \overline{\rho f} / \bar{\rho}$. The Smagorinsky constant is not allowed to take negative values while no upper bound is defined.

The sub-grid scale kinetic energy is calculated as:

$$k_{sgs} = c_I \Delta^2 \left| \tilde{S} \right|^2 \tag{10}$$

where the model parameter, c_I, is computed dynamically and varies locally in time and space:

$$c_I = \frac{\left\langle L_{kk} \right\rangle}{\left\langle \beta - a \right\rangle} \tag{11}$$

where the brackets correspond to averages computed as local averages of their face values with $L_{kk} = \bar{\rho}\tilde{u}_k\tilde{u}_k - \left(\overline{\rho u_k}\,\overline{\rho u_k} \right) / \bar{\rho}$, $\beta = 2\Delta^2 \bar{\rho} \left| \tilde{\tilde{S}} \right|^2$ and $a = 2\Delta^2 \bar{\rho} \left| \tilde{S} \right|^2$.

The constant Smagorinsky model [12], one of the standard models in FireFOAM, is also used for comparison purposes (Case 1). In the case of homogeneous isotropic turbulence, the Smagorinsky constant is estimated as $c_s \approx 0.17$ [13]. However, the Smagorinsky model is known to be too dissipative and the c_s constant is not universal. Rather, it depends on the flow configuration so that values of $c_s \approx 0.1$-0.2 [14] are often used in literature. A constant of $c_s = 0.1$ [15] is used in this study. The calculation of the sub-grid scale kinetic energy in the constant Smagorinsky model is based on the assumption that local equilibrium prevails and k_{sgs} is obtained from a balance equation as:

$$\bar{\rho}\left(\tilde{S} : B \right) + \frac{c_e \bar{\rho} k_{sgs}^{3/2}}{\Delta} = 0 \tag{12}$$

where ':' denotes the double product, $B = \frac{2}{3} k_{sgs} I - 2 c_k \sqrt{k_{sgs}} \Delta \tilde{S}_D$ is the sub-grid scale tensor, S_D is the deviatoric component of the strain rate tensor and $c_k = 0.05$, $c_e = 1.048$ [16] are two model constants. The sub-grid scale dissipation rate is calculated as:

$$\varepsilon_{sgs} = \frac{c_\varepsilon k_{sgs}^{3/2}}{\Delta} \tag{13}$$

The combustion model used employs a one-step, infinitely fast, irreversible chemical reaction, combined with the EDM model [3] for turbulence-chemistry interactions. Within the EDM model the fuel mass reaction rate is calculated as:

$$\overline{\dot{\omega}_F'''} = \bar{\rho} \frac{\min\left(\tilde{Y}_F, \tilde{Y}_{O_2} / s\right)}{\tau_{mix}} \tag{14}$$

where Y_F and Y_{O_2} are the fuel and oxygen mass fractions, respectively, s is the oxygen-fuel mass stoichiometric ratio and τ_{mix} is the reaction time scale. In the default implementation of the EDM model in FireFOAM (named EDM-A here), the reaction time scale model only considers molecular and turbulent diffusion, providing this way an estimate of the fuel-air mixing under laminar and turbulent flow conditions, respectively:

$$\tau_{mix} = \min\left(\underbrace{\frac{\Delta^2}{C_{diff}\alpha}}_{\tau_{lam}}, \underbrace{\frac{k_{sgs}}{C_{EDM}\varepsilon_{sgs}}}_{\tau_{turb}} \right) \tag{15}$$

where α is the laminar thermal diffusivity, $C_{diff} = 2$ and $C_{EDM} = 4$ are two model constants [17]. Nevertheless, the value for the C_{diff} constant is not universal and can vary depending on the case at hand (e.g., if laminar conditions are present in the flow). A sensitivity study on C_{diff} with values ranging between 2-10 was performed but did not reveal any influence of the parameter on the predicted results (effectively the laminar mixing time scale was not used). In the present study, a new reaction time scale model has been implemented (named EDM-B), in which the chemical time scale is compared with the mixing times for diffusion, sub-grid scale advection and buoyant acceleration, as proposed in [4]. The motivation behind applying the new reaction time scale model is to evaluate its predictive capabilities and to assess whether the scaling regime for coarse mesh resolution based on buoyant acceleration that it proposes is valid. This reaction time scale model is widely used in the fire community since it is a standard model in the CFD code Fire Dynamics Simulator (FDS) [18]. The detailed derivation of the model has been previously presented in [4] and is thus not repeated here. Within this model the reaction time scale is calculated as:

$$\tau_{mix} = \max\left[\tau_{chem}, \min\left(\tau_d, \tau_u, \tau_g, \tau_{flame} \right) \right] \tag{16}$$

where $\tau_{chem} = 10^{-10} s$ is the chemical time scale, relevant in cases of infinitely fast combustion, τ_d is the mixing time scale due to diffusion ($\tau_d = Sc_t \bar{\rho} \Delta^2 / (\mu + \mu_{sgs})$), τ_u is the mixing time scale due to advection ($\tau_u = \Delta / \sqrt{2k_{sgs}}$), τ_g is the mixing time scale due to buoyant

acceleration ($\tau_g = \sqrt{2\Delta / g}$), $\tau_{flame} = 10^{10}\, s$ presents the limit that the flame height poses on the reaction time scale, relevant to large scale fire simulations on coarse grids, Sc_t is the turbulent Schmidt number and g is the gravitational acceleration. For fires, which are buoyancy-driven flows, buoyant acceleration is expected to control the mixing at relatively coarse meshes, hence a time scale based on a constant acceleration that scales with the square root of the filter width is proposed [4]. Both τ_{chem} and τ_{flame} are effectively not considered in the current simulations but pose the extreme limits that τ_{mix} can take in the reaction time scale model.

A commonly used approach to model radiation is adopted, in which the radiative intensity is treated as a function of both spatial location and angular direction and is obtained by solving the radiative transfer equation (RTE) by the finite volume discrete ordinates model (fvDOM), assuming a non-absorbing, optically thin medium. Subsequently, the radiative heat fluxes in the enthalpy equation (Eq. (4)) are calculated as:

$$\nabla \cdot \overline{\dot{q}_r''} = \chi_r \overline{\dot{q}_c'''} \tag{17}$$

where χ_r is a constant global radiative fraction. This approach aims at bypassing the uncertainties related to modeling the radiation-turbulence interaction (RTI) as well as minimizing the dependency of the source term of the RTE on the filtered temperature, which can lead to significant errors in the calculations if coarse grids are employed.

Turbulent buoyant plume

The first test case (Case 1) aims at evaluating the dynamic Smagorinsky model and concerns the well-known experiments of a round axi-symmetric turbulent buoyant plume, reported by Shabbir et al. [5], generated by forcing a hot air jet vertically up into a quiescent environment. A nozzle, 6.35 cm in diameter, discharged the hot air with an average velocity of 0.98 m/s at 295 ºC. The experiments were conducted at a room temperature of 25 ºC in ambient pressure conditions. Centerline and radial velocity and temperature measurements were reported over a wide range of downstream distances from the source. Buoyant plumes are encountered in a wide range of engineering and environmental applications, hence, it is of great interest for fire safety engineers to be able to accurately predict their evolution and characteristics. In buoyant flows like this, the velocity and temperature plume profiles reach a self-similar profile further downstream and, if scaled, they can be represented by a single profile of Gaussian form [5].

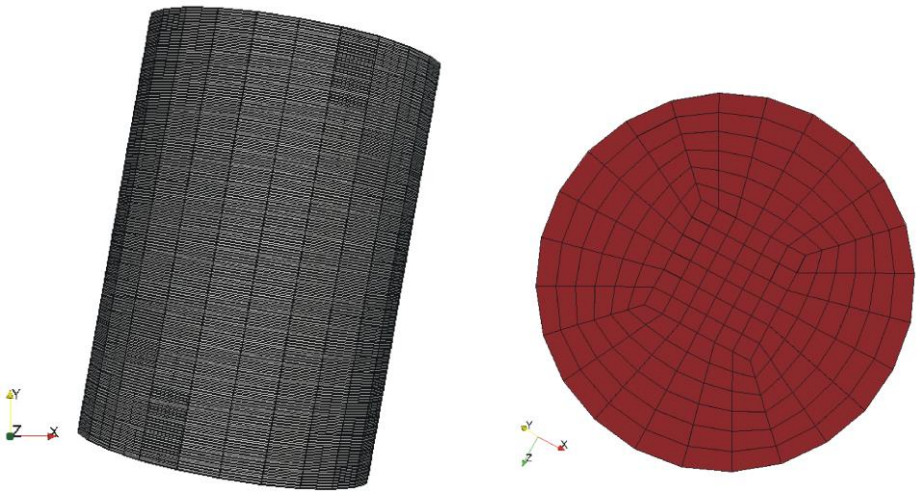

(a) (b)

Figure 1. Computational mesh used for Case 1. View of the (a) domain and (b) inlet.

A cylindrical computational domain of 15D x 20D (where D denotes the nozzle's diameter) is used to model the case, with 18 cells across the inlet (Fig. 1). The cell size is approximately 3.5 mm in the area of interest (centerline) and gradually increases radially to 2 cm at the sides of the computational domain. The total number of cells is then 432000. Constant velocity and temperature profiles are specified at the inlet corresponding to the experimentally reported values. Velocity perturbations are added through the synthetic method of random spots [19]. In order to excite the flow, a relatively high level of velocity fluctuations is necessary to be added at the inlet, as has been previously suggested by other authors (e.g. 20% in [15], [20]). In the current study, different levels of velocity perturbations were considered at the source, ranging from 0-20%, in order to examine their influence on the predicted flow field. The simulations were run for 200 s. Results averaged over the last 190 s were used to produce mean values.

A qualitative presentation of the differences in the flow field from the application of the constant and the dynamic Smagorinsky model is presented in Figure 2 for the case with no added fluctuations at the inlet (the other cases are similar and are omitted to avoid repetition). The structure of the plume with the constant Smagorinsky model is less turbulent and higher temperatures are evident further downstream when compared to the dynamic Smagorinsky. This leads to higher velocities on the centerline and delays the plume break-up at further locations from the source when the constant Smagorinsky model is applied. This is clearly portrayed below where a more quantitative comparison between the models is made.

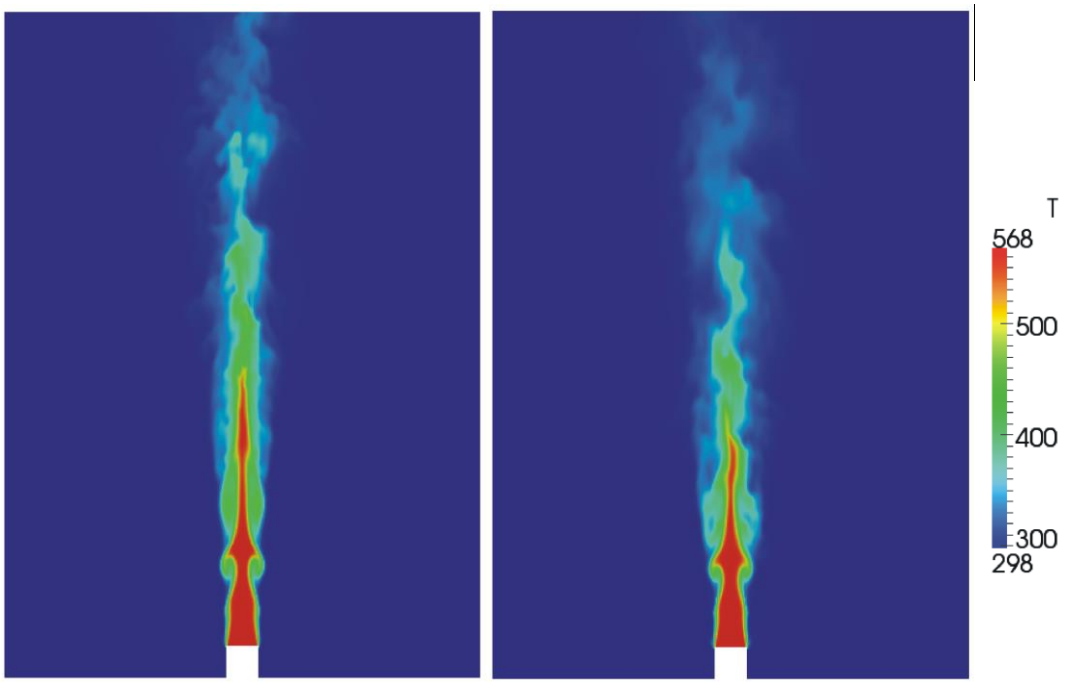

(a) (b)

Figure 2. Two-dimensional temperature contour with the (a) constant Smagorinsky and (b) dynamic Smagorinsky with no fluctuations at the inlet.

The averaged centerline axial velocities and temperatures for all the cases considered are displayed in Figure 3. The simulations performed without prescribing turbulent fluctuations at the inlet result in poor predictions and clearly demonstrate, as found in Zhou et al. [15], the necessity to account for turbulent inflow boundary conditions. If turbulent fluctuations are added at the inlet (10-20%), both the constant and dynamic Smagorinsky models produce, in the self-similarity region (i.e., y>10D), identical results, in excellent agreement with the experimental data. From Figure 3 it is also evident that the use of the dynamic Smagorinsky

model results in an earlier break-up of the plume, for the same amount of turbulent fluctuations at the inlet, with a lower peak in the axial velocity when compared to the constant Smagorinsky approach. In the absence of available experimental data near the inlet, no clear conclusions can be drawn as to which model performed better or worse. However, the maximum axial velocity (V_{max}≈1.75 m/s) obtained on the centerline with the dynamic Smagorinsky is in line with the numerical predictions by Zhou et al. [15]. The reason for the differences in the peak axial velocities between the constant and the dynamic models is the higher sgs viscosity with the constant Smagorinsky near the inlet, shown in Figure 4, making the effective viscosity higher and delaying its break-up to a location further downstream. Overall, the ratio of sgs to laminar viscosity for all cases remains below 0.65, indicating that the contribution from the turbulence model is not significant and sgs quantities remain comparable to the laminar quantities.

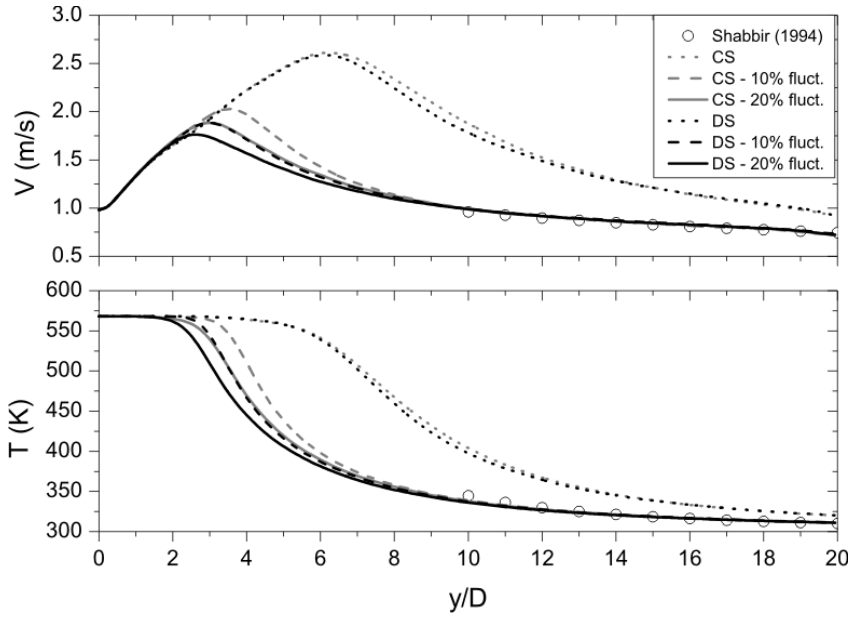

Figure 3. Variation of mean centerline axial velocity (top) and temperature (bottom) in the simulations. CS: Constant Smagorinsky (c_s=0.1), DS: Dynamic Smagorinsky.

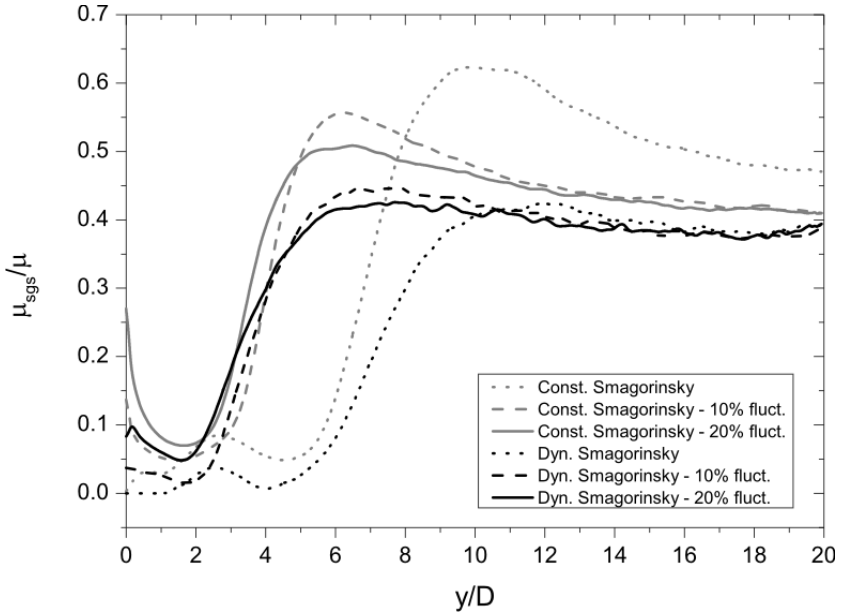

Figure 4. Ratio of sub-grid scale to laminar viscosities in the simulations.

Figure 5 shows a good agreement between the simulations and the experiments for the predicted self-similarity profiles of axial velocity and temperature at three heights above the inlet (i.e., 10D, 14D and 18D). The results displayed confirm the good predictive capabilities of the dynamic Smagorinsky model when applied to a turbulent buoyant plume scenario which has resembling characteristics of a fire scenario (i.e., buoyancy driven flow). Although the results obtained using the dynamic model are very similar to the static model in the self-similar region for the case at hand, the former approach has the significant advantage of self-adjusting the sgs viscosity. Therefore, no calibration or sensitivity analysis on the choice of the turbulence model constant is required.

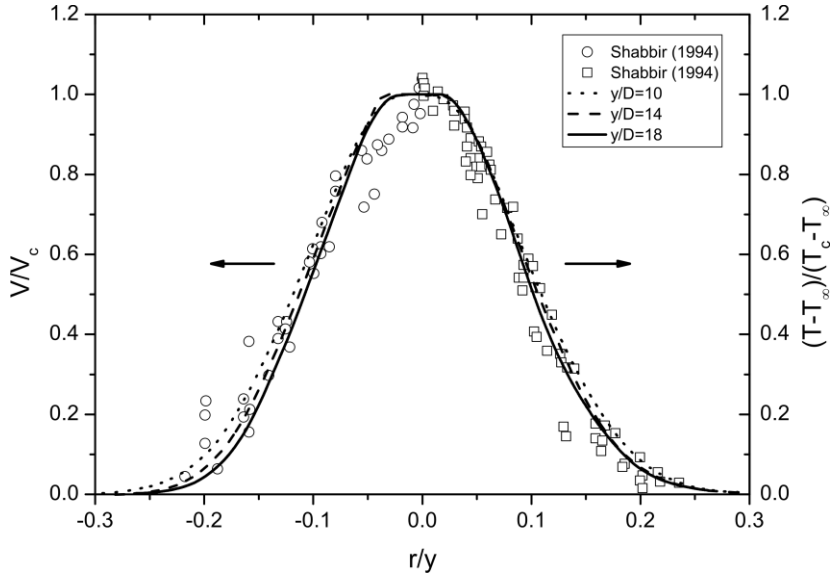

Figure 5. Radial profiles of normalized axial velocity (left) and temperature (right) with the dynamic Smagorinsky (20% fluctuations).

Small scale CH_4 fire plumes

The second case (Case 2) aims at evaluating the EDM-B model and considers the small-scale CH_4 fire plume experiments (14.4-57.5 kW) by McCaffrey et al. [6]. A square burner of dimensions 0.3 m x 0.3 m was used in the experiments and a complete set of centerline temperatures and velocities were reported at various downstream locations from the fire source. It is worth noting, however, that the experimental data were not corrected for thermocouple radiation, effectively under-predicting the flame temperatures by 20% [6].

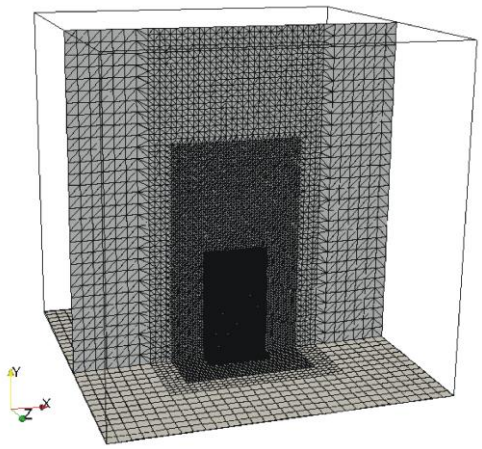

Figure 6. Computational mesh used for Case 2.

A cubic box of 3 m x 3 m x 3 m is used as a computational domain, shown in Figure 6. A local grid refinement strategy was employed, defining four regions: the cell size varies from 1.25 cm in the areas of interest (flame and intermittent regions) to 2.5 cm (plume region) and 5-10 cm (top and sides of the domain). The total number of cells used is approximately 540000. The corresponding mass flow rate was applied at the inlet with a fixed value of 20 ºC for temperature. A radiative fraction of $\chi_r = 20\%$ [6] is used in all numerical simulations. The simulations were run for 50 s. Results are averaged over the last 45 s to produce mean values.

Figure 7 presents the instantaneous temperature plots for three of the tests simulated (14.4 kW, 33.0 kW and 57.5 kW). The three regions of a typical fire plume can be clearly distinguished: the flame region where continuous flames are present, the intermittent region where the flames are pulsating and the plume region where combustion products are convected downstream. As expected, higher flame temperatures and more turbulent structures are evident with higher heat release rate, as well as an increase of the predicted flame height.

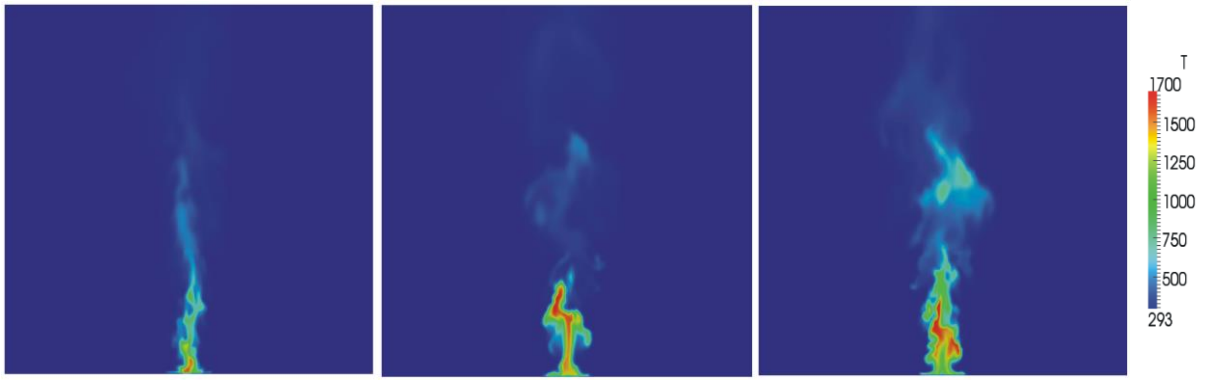

Figure 7. Instantaneous two-dimensional temperature contour plot with the dynamic Smagorinsky for (a) 14.4 kW (b) 33.0 kW and (c) 57.5 kW with EDM-B.

The variation of the predicted centerline temperature rise and velocity using the dynamic Smagorinsky and the two EDM models, EDM-A and EDM-B, is presented in Figure 8. McCaffrey observed that if the downstream distance, *y*, from the fire source was scaled with $\dot{Q}^{2/5}$ then the sets of data for the centerline temperature rise and the centerline velocity normalized by $\dot{Q}^{1/5}$, each one collapsed onto a single curve, independently of the heat release rate. McCaffrey's correlations are presented as solid grey lines, while the dashed line corresponds to a 20% correction of the centerline temperature rise to account for the fact that the experimental data were not corrected for thermocouple radiation. The current simulations closely follow McCaffrey's scaling proposal and all curves almost collapse onto a single curve in the case of the centerline temperature rise, having an almost zero slope in the flame region ($y/\dot{Q}^{2/5} < 0.08$), a -1 decay slope in the intermittent region ($0.08 < y/\dot{Q}^{2/5} < 0.2$) and a -5/3 decay slope in the plume region ($y/\dot{Q}^{2/5} > 0.2$). A similar good agreement in the scaling is observable for the predicted centerline velocities. The simulations with the EDM-A model yield systematically higher temperatures than the EDM-B model in the flame and intermittent regions. Deviations up to 200 K are observed. Nevertheless, in the plume region, temperatures are very similar. Similar observations are made by examining the predicted centerline velocities with the two EDM models.

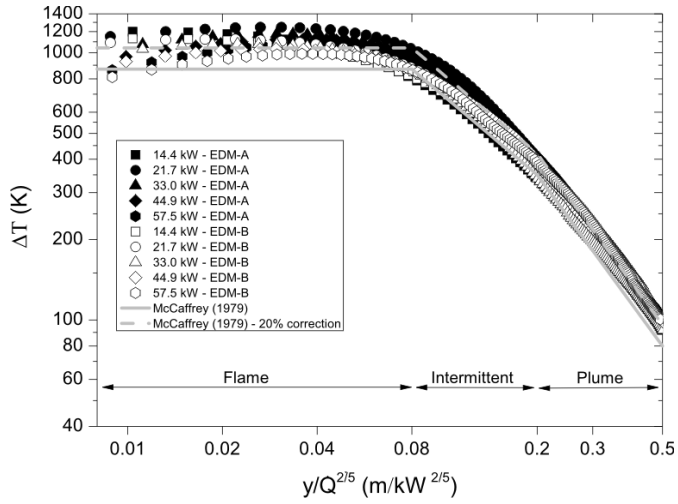

(a)

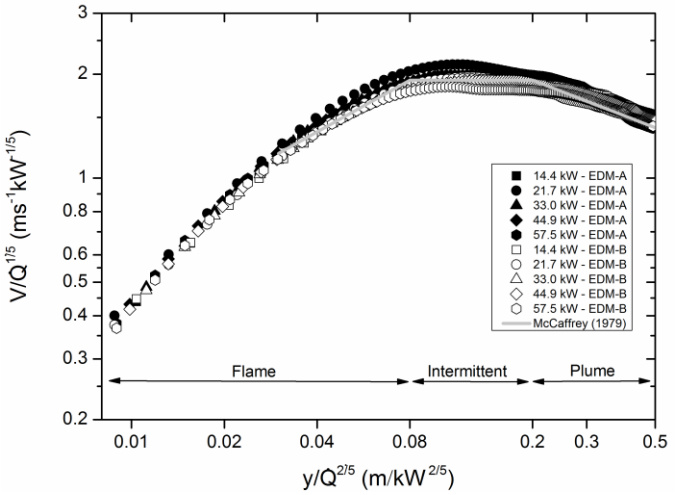

(b)

Figure 8. Variation of centerline (a) temperature rise and (b) axial velocity with the dynamic Smagorinsky. EDM-A: Eq. (14) and Eq. (15), EDM-B: Eq. (14) and Eq. (16).

The reason for the differences could be attributed to the absence of buoyant mixing in the EDM-A model in FireFOAM, which can be important in the case of fires, but also due to the different definition/derivation of the turbulent mixing time scale between EDM-A (τ_{turb}) and EDM-B (τ_u). It is worth noting that the different derivation of the two reaction time scale models (or the different implicit use of model constants while deriving the two models) eventually leads to significant differences in the resulting mixing time scale due to turbulence/advection here named τ_{turb} and τ_u. The use of typical values such as $C_{EDM} = 4$ and $c_e = 1.048$ (used in the present study) leads to $\tau_u \approx \tau_{turb}$ (depending also on the calculated values of k_{sgs}). The resulting τ_{mix} values, shown in Figure 9(a), are significantly lower in the case of EDM-A than those of EDM-B, implying that mixing between fuel and oxidizer is much faster with the EDM-A model. Thus, these lower τ_{mix} values with EDM-A enhance combustion and produce higher temperatures in the flame and intermittent regions of the fire plumes. The time scales due to diffusion (τ_{lam} in EDM-A and τ_d in EDM-B) are significantly higher compared to the other time scales in both models and are effectively never considered for the cases at hand. Only the turbulent time scale, τ_{turb}, is considered in the EDM-A model while in the EDM-B model only the mixing times for buoyant acceleration, τ_g (flame region),

and sub-grid scale advection, τ_u (flame-intermittent-plume regions), are used. Figure 9(b) presents the resulting fuel mass reaction rates with the EDM-A and EDM-B models. As expected, based on the mixing times scales, the reaction rates in the case of the EDM-A model are significantly higher, which in turn enhances combustion and results in higher temperatures in the flame and intermittent regions of the fire plumes (Figure 8(a)).

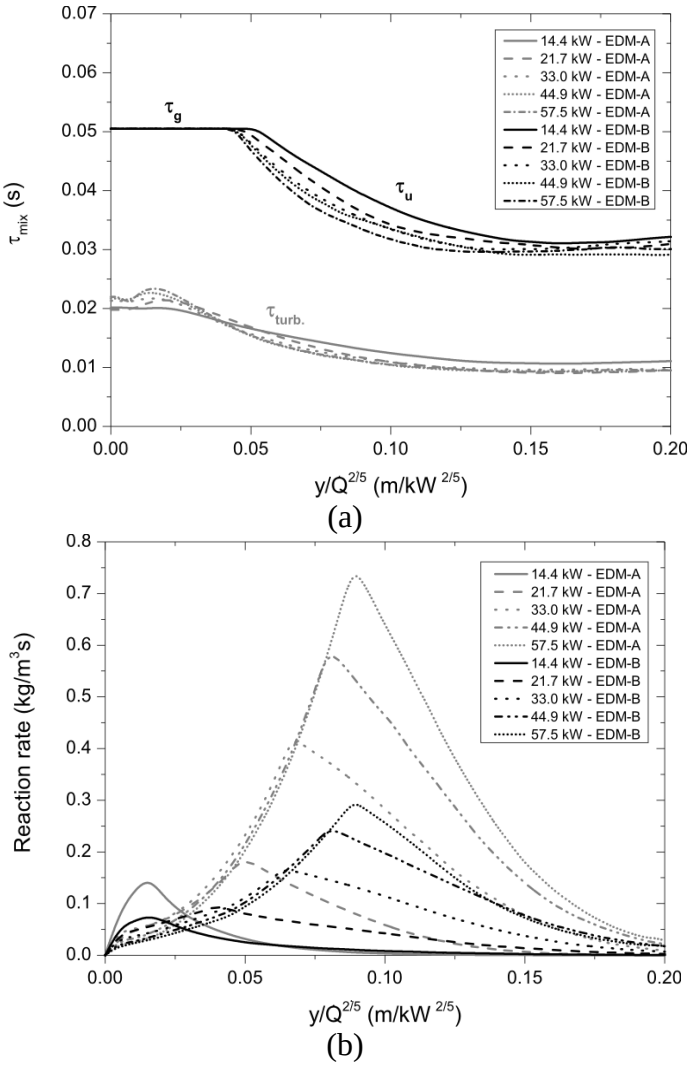

Figure 9. Centerline evolution of the (a) mixing time scale and (b) fuel reaction rate with the dynamic Smagorinsky. EDM-A: Eq. (15) and Eq. (16), EDM-B: Eq. (15) and Eq. (17).

Conclusions

Recent developments, namely the implementation of the dynamic Smagorinsky model [2] and the Eddy Dissipation Model with multiple reaction time scales [4], in the gas phase models of the CFD code FireFOAM were presented. The newly implemented models were evaluated against two well-characterized experimental test cases, involving turbulent buoyant plumes and small-scale CH_4 fire plumes. The deviations between the experimental data and results with the new reaction time scale model employed, which considers mixing times for diffusion, sgs advection and buoyant acceleration, were slightly lower compared to results obtained with the standard reaction time scale model in FireFOAM, which considers molecular and turbulent mixing only. The main conclusion, though, is that this is achieved without the need for user-input model parameters for turbulence in the gas phase. Overall, very good quantitative and qualitative agreement between the simulations and the different

experimental test cases considered was observed with the application of the newly implemented models. The implementation and evaluation of these models aims to supplement the currently available models in FireFOAM and to enhance the predictive capabilities of the code towards simulating fire-related scenarios.

Acknowledgements
This research has been funded by Ghent University (Belgium) through GOA project BOF16/GOA/004. Dr. Tarek Beji is a post-doctoral fellow of the Fund of Scientific Research - Flanders (Belgium) (FWO Vlaanderen).

References

[1] Hurley, M.J., Rosenbaum, E.R., *Performance-Based Fire Safety Design*, CRC Press, 2015.
[2] Moin, P., Squires, K., Cabot, W., Lee, S., "A dynamic subgrid-scale model for compressible turbulence and scalar transport", *Phys. Fluids A* 3: 2746-2757 (1991)
[3] Magnussen, B.F., Hjertager, B.H., "On Mathematical Models of Turbulent Combustion with Special Emphasis on Soot Formation and Combustion", *Proc. Comb. Inst.* 16: 719-729 (1977)
[4] McDermott, R., McGrattan, K., Floyd, J., "A Simple Reaction Time Scale for Under-Resolved Fire Dynamics", *Fire Safety Science* 10: 809-820 (2011)
[5] Shabbir, A., George, W.K., "Experiments on a round turbulent buoyant plume", *J. Fluid Mech.* 275: 1-32 (1994)
[6] McCaffrey, B.J., "Purely Buoyant Diffusion Flames: Some Experimental Results", *NBSIR 79-1910*, National Bureau of Standards, 1979.
[7] Wang, Y., Chatterjee, P., de Ris , J.L., "Large Eddy Simulation of Fire Plumes", *Proc. Comb. Inst.* 33: 2473-2480 (2011)
[8] Poinsot, T., Veynante, D., *Theoretical and Numerical Combustion*, Edwards, 2012.
[9] Sutherland, W., "The viscosity of gases and molecular force", *Philosophical Magazine.* 36: 507-531 (1893)
[10] Prausnitz, J.M., Reid, R.C., Sherwood, T.K., *The Properties of Gases and Liquids*, McGraw-Hill, 1977.
[11] Burcat, A., *Thermochemical Data for Combustion Calculations*, J. Wiley & Sons, 1984.
[12] Smagorinsky, J., "General Circulation experiments with the primitive equations I. The basic experiment", *Monthly Weather Review* 91: 99-164 (1963)
[13] Pope, S.B., *Turbulent Flows*, Cambridge University Press, 2000.
[14] Garnier, E., Sagaut, P., *Large Eddy Simulation for Compressible Flows*, Springer, 2009.
[15] Zhou, X., Luo, K.H., Williams, J.J.R. "Large-eddy simulation of a turbulent forced plume", *Eur. J. Mech. B-Fluids* 20: 233-254 (2001)
[16] Fureby, C., Tabor, G., Weller, H.G., Gosman, A.D., "A comparative study of sub-grid scale models in homogeneous isotropic turbulence", *Phys. Fluids* 9: 1416-1429 (1997)
[17] Ren, N., Wang, Y., Vilfayeau, S., Trouvé, A., "Large Eddy Simulation of Propylene Turbulent Vertical Wall Fires", *7th International Seminar on Fire and Explosion Hazards*, Providence, 2013.
[18] McGrattan, K., McDermott, R., Floyd, J., Hostikka, S., Forney, G., Baum, H., Computational fluid dynamics modelling of fire, Int. J. Comput. Fluid D. 26: 349-361 (2012)
[19] Kornev, N., Hassel, E. "Method of random spots for generation of synthetic inhomogeneous turbulent fields with prescribed autocorrelation functions", *Comm. Numer. Meth. En* 23: 35-43 (2007)
[20] Ma, T., "Large-eddy simulation of variable density flows", *PhD thesis*, University of Maryland, 2006.